Revisiting the GW approach to d- and f-electron oxides

Hong Jiang*

Beijing National Laboratory for Molecular Sciences, College of Chemistry and Molecular Engineering, Peking University, 100871 Beijing, China

(Received 17 April 2018; published 21 June 2018)

Accurate description of electronic band structure of strongly correlated d- or f-electron materials has been regarded as a great challenge for first-principles electronic structure theory. Previous theoretical studies based on the GW approach has met mixed success, and in particular, the one-short (G_0W_0) or partially self-consistent (GW_0) approaches with the local or semilocal density functional approximations plus the Hubbard U correction (GW@LDA+U) as the reference systematically underestimate the binding energies of occupied d or f states. In this work we have investigated quasiparticle electronic band structures of a series of d- or f-electron oxides including late transition metal mono-oxides (TMO, TM = Mn, Fe, Co, and Ni), La_2O_3, CeO_2, Ce_2O_3, and UO_2. It is shown that a large part of the errors observed in previous GW studies can be attributed to numerical errors related to the inaccuracy of unoccupied states and the incompleteness of the summation of states, which can be effectively overcome by including high-energy local orbitals (HLOs) in the linearized augmented plane waves (LAPW) framework.

DOI: 10.1103/PhysRevB.97.245132

I. INTRODUCTION

Electronic band structure is one of the most important properties of a material, and plays a crucial role in determining its applications in electronics, photoelectronics, photovoltaics, and photocatalysis [1–4]. Accurate and efficient theoretical prediction of electronic band structure of materials is therefore a central task for first-principles materials research. In recent decades, many-body perturbation theory in the GW approximation [5], often implemented as a correction to Kohn-Sham density functional theory (KS-DFT) in the local density approximation (LDA) or the generalized gradient approximation (GGA), hence termed as G_0W_0, has become the most accurate first-principles approach to theoretical description of electronic structure of semiconductors without any empirical input [1,6–9]. In practice, the GW method has been implemented in various different schemes, including using pseudopotentials (PP) with the plane wave (PW) [6,7,10] or local atomic basis [11,12], the projector augmented wave (PAW) [13–15], the linearized augmented plane waves (LAPW) or the muffin-tin orbital (LMTO) methods [16–27], and all-electron numerical atomic basis [28]. For many typical sp semiconductors, different implementations of the GW approach give essentially similar results, in spite of different treatments of core-valence interactions and/or numerical basis. However, recent studies [26,27,29–32] have revealed that the numerical accuracy of the GW implementation is more difficult to achieve for some systems. For ZnO in particular, the "standard" G_0W_0 scheme, i.e., using typical computational parameters with LDA or GGA as the starting point, either in the PP-PW, PAW, or LAPW framework, can underestimate the fundamental gap by nearly 1 eV, which is significantly larger than the typical errors (0.1–0.2 eV) observed in other sp semiconductors. This error used to be attributed to theoretical limitations of the LDA or GGA-based G_0W_0 approach, but now it has been clarified that the numerical accuracy of the GW implementation is the true reason for such dramatic errors [26,27,31]. In particular, for systems like ZnO, both the accuracy of unoccupied states, and the completeness in the summation of unoccupied states, play important roles in determining the overall accuracy of the GW results [26]. The first factor is affected not only by the completeness of the numerical basis used to expand Kohn-Sham orbitals, but also by the accuracy of a pseudopotential to reproduce scattering properties of the full potential at high energies, or by the linearization error in the LAPW basis for states far away from the Fermi level. When implemented in the LAPW framework, the two issues can be solved by introducing additional high-energy local orbitals (HLOs) as an extension of the standard LAPW basis [31,33], and considering all unoccupied states available in the GW calculations [26]. When implemented in the PAW framework, the two problems above can be overcome by using specially tailored and approximately norm-conserving PAW pseudopotentials, which have additional projectors at higher energies, and in addition, extrapolating the calculated GW band gaps to an infinite number of unoccupied states [32,34]. One would expect that similar treatments can also be used in the GW implementation with norm-conserving or ultrasoft pseudopotentials, which, however, has not been reported, as far as we know.

Based on a systematic investigation of tens of typical sp semiconductors using GGA-based G_0W_0 or GW_0 approach implemented in the HLOs-extended LAPW (LAPW+HLOs) basis [26], we have found that only relatively few cases, with ZnO and LiF as two notable examples, are significantly affected by the accuracy of GW implementation, as far as fundamental band gaps are concerned. It is then of great interest to investigate the effects of using LAPW+HLOs for GW

*Corresponding author: jianghchem@pku.edu.cn

calculations of d- or f-electron systems. For that purpose, we readdress the performances of the GW approach to d- and f-electron oxides by considering a set of typical transition metal, lanthanide, and actinide oxides. As in our previous studies [35,36], we use the Hubbard U-corrected LDA or GGA as the starting point for G_0W_0 or GW_0 calculations, an approach that has been widely used in GW studies of strongly correlated materials [35–42]. Our previous studies of lanthanide oxides [35,37] show that although LDA+U based G_0W_0 can well reproduce the characteristic features in the evolution of the band gap of Ln_2O3 as a function of the number of $4f$ electrons, the binding energy of occupied $4f$ states tends to be significantly underestimated with respect to the energy of O-$2p$ derived valence states. It was attributed to the intrinsic theoretical limitation of the GW@LDA+U approach [35,36], but with the improved numerical accuracy of using the LAPW+HLOs basis, we will show that the real origin for that is of numerical nature.

The paper is organized as followings. Section II presents some computational details of our calculations. In Sec. III we present systematic investigations of the effects of including HLOs in GW calculations for typical transition metal oxides, lanthanide, and actinide oxides, and compare the numerically converged results with experimental data when available. Section IV summarizes the main findings of this work and closes the paper with some general remarks.

II. COMPUTATIONAL DETAILS

We use the all-electron GW method implemented in the HLOs-extended LAPW basis. The detailed formalism used in our implementation has been presented in our previous work [26], and is therefore not repeated here. The essence of including HLOs in the LAPW-based GW calculation is as follows. The standard LAPW basis is most accurate to describe Kohn-Sham orbitals for occupied (valence band) states or low-lying unoccupied (conduction band) states not far away from the Fermi energy, but has significant linearization error for the description of states far away from the Fermi level [20,31,33,43]. For GW and other theoretical approaches, e.g., the random phase approximation (RPA) method for the ground state total energy [44,45], which depend on the summation of all unoccupied states, both the accuracy of unoccupied states and the completeness of the summation of states play a crucial role in the numerical accuracy of calculated results [26]. In the LAPW framework, an effective way to take into account both factors is to include an adequate number of additional local orbitals energetically higher than normal valence states [31,33], which, together with the original LAPW basis, is termed as LAPW+HLOs [26].

Our previous analysis of ZnO in Ref. [26] indicates that using the LAPW+HLOs basis can improve the GW results in two aspects: (1) unoccupied Kohn-Sham orbitals with energy up to the plane-wave energy cutoff, typically around 20 Ry or higher, are much more accurately represented, which can have significant effects on the numerical accuracy of GW results for systems like ZnO, and (2) the inclusions of HLOs, which can have energy as high as 100–200 Ry, introduces a few hundred extremely high-energy unoccupied states in the same energy regime as HLOs, and the consideration of these states can effectively lead to numerically converged GW band gaps without using the extrapolation treatment as required in PAW-based GW calculations [32,34].

The quality of the LAPW+HLOs basis can be characterized by the additional number of nodes in the radial function of highest energy local orbitals, denoted as $n_{\rm LO}$, and the maximum angular quantum number of local orbitals, denoted as $l_{\rm max}^{\rm (LO)}$. Based on our previous study of typical sp systems [26], we have found that the dependence of the numerical accuracy of GW results on $n_{\rm LO}$ and $l_{\rm max}^{\rm (LO)}$ is related to the nature of the system concerned, and therefore we will check the convergence of GW calculation with respect to $n_{\rm LO}$ and $l_{\rm max}^{\rm (LO)}$ for each type of system considered in this work.

We will present numerical results for a series of typical d- and f-electron oxides, including later transition metal oxides TMO (TM = Mn, Fe, Co, and Ni) with partially occupied $3d$ shell, lanthanide or actinide compounds with empty (CeO_2 and La_2O_3), and partially occupied f shell (Ce_2O_3 and UO_2). For TMO we consider the type-II antiferromagnetic (AFM) ordering along the (111) direction [46]. For Ce_2O_3 we consider the AFM phase in which two Ce atoms in the hexagonal unit cell have antiparallel magnetic momenta [37]. For UO_2 we consider the AFM ordering along the (001) direction, as often considered in previous theoretical studies of this compound [47–50]. We use experimental crystal structures, taken from Ref. [51] for MnO, FeO, CoO, and NiO, Ref. [52] for CeO_2, La_2O_3 and Ce_2O_3, and Ref. [53] for UO_2, in all calculations to facilitate the comparison between theory and experiment.

Similar to our previous work [26], we are going to present two types of numerical results. When investigating how GW band gaps are affected by including increasingly more HLOs (as characterized by $n_{\rm LO}$ and $l_{\rm max}^{\rm (LO)}$), we present the G_0W_0 results obtained with a small number of $\mathbf{k}$ points ($2\times2\times2$ for NiO and CeO_2, and $2\times2\times1$ for Ce_2O_3). We also present numerical results that are obtained by using a significantly larger $\mathbf{k}$ mesh to ensure the numerical error related to N_k of less than 0.05 eV. In particular, we use the $\mathbf{k}$ mesh of $4\times4\times4$ for TMO, $3\times3\times2$ for La_2O_3 and Ce_2O_3, $4\times4\times4$ for CeO_2, and $4\times4\times3$ for UO_2.

We use $n_{\rm LO}=0$ to denote the default LAPW basis in the recent version of WIEN2k [54], which is actually a mixture of the APW+lo basis [55] for the valence states, the ordinary LAPW basis for higher l channels up to $l_{\rm max}=10$, and additional LOs for semicore states if present [54]. By default we add high-energy local orbitals to the LAPW basis with the angular momentum l up to $l_{\rm max}^{\rm (LO)}={\rm Min}(3,l_{\rm max}^{\rm (v)}+1)\equiv l_{\rm max}^{\rm (LO)}({\rm def})$, with $l_{\rm max}^{\rm (v)}$ being the largest l of valence orbitals for each element, e.g., $l_{\rm max}^{\rm (v)}=1$ and 2 for O and Ni, respectively [33,43]. The convergence with respect to both $n_{\rm LO}$ and $l_{\rm max}^{\rm (LO)}$, the latter being represented by $\Delta l_{\rm LO}$ in $l_{\rm max}^{\rm (LO)}\equiv l_{\rm max}^{\rm (v)}+\Delta l_{\rm LO}$, is going to be investigated in detail. Some additional information about computational parameters used in our calculations is presented in Table S1 in the Supplemental Material [56].

We will present GW results in both G_0W_0 and GW_0 schemes, in which Kohn-Sham orbital energies and wave functions calculated with the Perdew-Burke-Ernzerhof (PBE) [57] GGA plus the Hubbard U correction (PBE+U) are used as the input to calculate one-body Green's function G and screened Coulomb interaction W. The values of the on-site Coulomb and exchange interaction parameters (the Hubbard

U and Hund J) are determined by using the constrained DFT approach [58] in the LAPW implementation [37,59].

We note that for CeO_2 and La_2O_3 with an empty $4f$ subshell, the Hubbard U correction is not necessary in some sense, since standard LDA or GGA predicts qualitatively correct insulating ground state, although with a significantly underestimated band gap, and G_0W_0 or GW_0 based on LDA or GGA can already lead to a rather accurate description [35,37]. Nevertheless, the inclusion of the Hubbard U correction in LDA/GGA can often lead to further improvement in the G_0W_0 or GW_0 description of these compounds [36,41]. The default LAPW basis ($n_{\mathrm{LO}} = 0$) is used in the PBE(+U) self-consistent field (SCF) calculations, since the effects of including HLOs in SCF calculations are negligible, as we have shown previously [26].

For the systems considered in this work, relativistic effects are expected to be significant, especially for f-electron oxides like UO_2. While scalar relativistic effects are fully taken into account at the PBE level, spin-orbit coupling (SOC) is not considered due to the limitation of our current GW implementation. We have investigated the effects of considering SOC on the band structure of f-electron oxides in the PBE+U calculations, in which SOC is considered by the second-variational approach [60]. A comparison of PBE+U DOS of UO_2, with and without SOC, is presented in Fig. S1 in the Supplemental Material [56], which shows that the consideration of SOC has some noticeable but weak effects on the band structure of UO_2. We can therefore expect that the consideration of SOC will not significantly change the GW electronic band structure properties presented in this paper.

III. RESULTS AND DISCUSSIONS

A. Transition metal oxides MO (M = Mn, Fe, Co, and Ni)

We first consider later transition metal mono-oxides TMO (TM = Mn, Fe, Co, and Ni). These are prototypical strongly correlated systems that are widely used as the testbed for first-principles approaches for strongly correlated systems [46,68,71–74].

We use NiO as the representative to investigate the effects of including HLOs on the GW band gaps. Figure 1 shows the convergence of the G_0W_0@PBE band gap of NiO with respect to n_{LO} and $l_{\mathrm{max}}^{(\mathrm{LO})}$. Compared to what is found in ZnO [26] and other d^{10} compounds [75], the effects of including HLOs on the G_0W_0 band gap of NiO are significantly weaker. The band gap increases only by about 0.3 eV as n_{LO} increases from 0 to 5, and increasing $l_{\mathrm{max}}^{(\mathrm{LO})}$ has also a mild effect on the GW band gap. On the other hand, the inclusion of HLOs can push the valence band maximum (VBM) towards lower energy dramatically as the value of $\Delta\mathcal{E}_{\mathrm{VBM}}$ evolves from being slightly positive (0.05 eV for $n_{\mathrm{LO}} = 0$) to strongly negative (-1.21 eV for $n_{\mathrm{LO}} = 5$ and $l_{\mathrm{max}}^{(\mathrm{LO})} = l_{\mathrm{max}}^{(\mathrm{v})} + 6$), which indicates that the GW-corrected ionization potential [24] of NiO increases by nearly 1.3 eV when HLOs are considered. The different effects of adding HLOs on E_{g} and $\Delta\mathcal{E}_{\mathrm{VBM}}$ are consistent with the fact that both VBM and conduction band minimum (CBM) states have strong Ni-3d characters, including HLOs can significantly push both VBM and CBM towards lower energy and therefore the band gap changes less dramatically than the VBM energy.

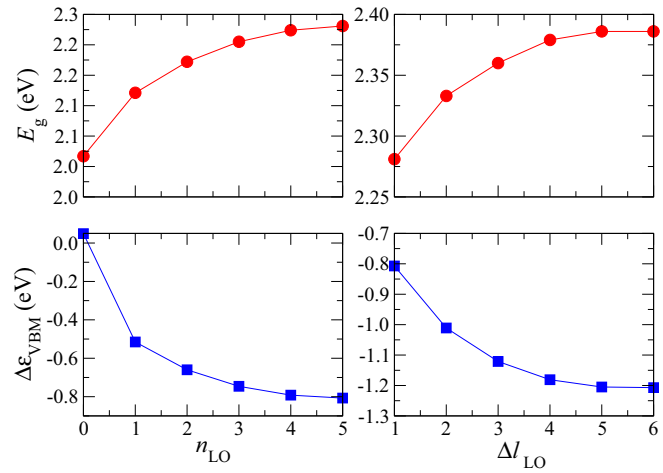

FIG. 1. Convergence of the G_0W_0@PBE band gap (E_{g}, upper panels) and the quasiparticle correction to the valence band maximum (VBM) ($\Delta\mathcal{E}_{\mathrm{VBM}}$, lower panels) of NiO in its AFM-II structure (using $N_k = 2\times2\times2$) as a function of n_{LO} [left panels, with $l_{\mathrm{max}}^{(\mathrm{LO})} = l_{\mathrm{max}}^{(\mathrm{LO})}(\mathrm{def})$] and Δl_{LO} in $l_{\mathrm{max}}^{(\mathrm{LO})} = l_{\mathrm{max}}^{(\mathrm{v})} + \Delta l_{\mathrm{LO}}$ (right panels, with $n_{\mathrm{LO}} = 5$), respectively.

Table I collects the band gaps of all later transition metal oxides obtained from PBE+U, G_0W_0, and GW_0@PBE+U approaches, obtained with a fine $4\times4\times4$ **k** mesh. Experimental results for the fundamental band gaps of these compounds are also collected for comparison. In general the band gaps from GW_0 are slightly larger than those from G_0W_0, which are included for the purpose of completeness. We will mainly discuss the GW_0 results henceforth. Comparing the GW_0 band gaps obtained with standard LAPW ($n_{\mathrm{LO}} = 0$) and LAPW+HLOs ($n_{\mathrm{LO}} = 5, l_{\mathrm{max}}^{(\mathrm{LO})} = l_{\mathrm{max}}^{(\mathrm{v})} + 4$), we can clearly see that overall including HLOs tends to increase the fundamental gap, but the magnitude of change is system dependent, which can be well interpreted in terms of the different characters of VBM and CBM in different systems. For example, the effects of HLOs are relatively weak for the GW band gap of FeO, which can be attributed to the fact that both VBM and CBM have strong Fe-3d characters, and including HLOs push both VBM and CBM states towards lower energy, and therefore leads to an overall small change of the fundamental band gap. For MnO, on the other hand, which has a fully filled (empty) spin-majority (minority) 3d shell, the VBM is mainly contributed by oxygen-2p orbitals, and the CBM is mainly of Mn-4s characters. In that case, the inclusion of HLOs pushes the VBM towards lower energy more strongly than it does CBM, and therefore the band gap of MnO increases strongly by about 1 eV.

When comparing with experiment, some caution has to be taken considering the uncertainty related to how the band gap is measured and extracted from experimental data. The band gaps of transition metal oxides are especially difficult to measure accurately, not only because it is more difficult to grow high-quality single crystals compared to common sp semiconductors, but also because the electronic excitations involved in photoelectron spectroscopy or optical absorption spectroscopy are often much more complicated, and therefore the extraction of the band gap from those measurements is

TABLE I. Band gaps of late transition mono-oxides from PBE+U and GW_0@PBE+U at different levels of numerical accuracy compared to experiment. The columns with "LAPW" are the results obtained from using the default LAPW basis ($n_{\rm LO} = 0$), and those with "LAPW+HLOs" are the results obtained with $n_{\rm LO} = 5$, $l_{\rm max}^{\rm (LO)} = l_{\rm max}^{\rm (v)} + 4$. The values of U and J, estimated based on the constrained density functional theory calculations, are taken from Ref. [36].

			G_0W_0		GW_0			
System	U, J	PBE+U	LAPW	LAPW+HLOs	LAPW	LAPW+HLOs	Expt.	Previous GW studies
MnO	4.7, 0.8	1.62	2.33	3.32	2.51	3.69	3.9 ± 0.4,[a] 4.1[b]	3.4,[g] 3.5,[h] 4.39,[i], 4.03[j]
FeO	4.8, 0.9	1.05	1.47	1.71	1.47	1.87	2.4[c]	2.2,[g] 2.32[j]
CoO	5.1, 0.9	2.19	2.42	3.42	2.30	3.76	2.5 ± 0.3,[d] 2.6,[b] 3.6 ± 0.5[e]	3.4,[g] 4.78,[i], 3.02[j]
NiO	5.2, 0.9	3.08	4.06	4.65	4.09	4.83	4.3,[f] 4.0[b]	4.7,[g] 4.8,[h] 5.0,[i] 3.60[j]

[a]Reference [61].
[b]Reference [62].
[c]Reference [63].
[d]Reference [64].
[e]Reference [65].
[f]Reference [66].
[g]G_0W_0@HSE implemented in the PAW from Ref. [67].
[h]QPscGW implemented in the LMTO basis from Ref. [68].
[i]QPscGW implemented in the PAW basis from Ref. [69].
[j]Self-consistent model GW implemented in the LAPW basis from Ref. [70].

highly nontrivial. In many cases, the band gap is extracted from experimental spectral data, typically obtained by combining x-ray photoelectron spectroscopy (XPS) and bremmsstrahlung isochromat spectroscopy (BIS) measurements [61,64,76], by assigning band edges in a quite ad hoc manner. For example, van Elp *et al.* [64] determines the band gap of CoO by taking the valence band maximum at 50% of the intensity increase in the XPS data and the conduction band minimum at 10% intensity increase in the BIS data, based on the estimated resolution of XPS and BIS spectral data. That explains the fact that the experimental band gaps of these compounds usually scatter in a considerable range, and the comparison between theory and experiment has to be done in a careful way. The GW_0 band gap for MnO with the default LAPW basis is about 2.5 eV, which is smaller than the experimental value by about 1.4 eV. After considering the HLOs, the GW_0@PBE+U predicts the fundamental band gap of MnO in good agreement with experiment. For FeO, the calculated band gap either at the G_0W_0 or GW_0 level is considerably smaller than the experimental value of 2.4 eV, but the inclusion of the HLOs significantly reduces the discrepancy between theory and experiment. For CoO and NiO, the band gaps from GW_0 with the LAPW+HLOs basis appear to be overestimated compared to the experimental data.

In Table I we have also collected the results from some recently published studies of the TMOs by the GW approach implemented in different schemes, which also exhibits significant scattering. It is interesting to note that our GW_0 results with LAPW+HLOs are close to those from the quasiparticle self-consistent GW (QPscGW) approach [68] implemented in the linear muffin-tin orbital (LMTO) [68] or PAW [69]. That indicates that improving numerical accuracy in the GW implementation and incorporating quasiparticle self-consistency both tend to increase the band gap for later TMOs, and it implies that QPscGW, when implemented with higher numerical accuracy, could lead to even more greatly overestimated band gaps of TMOs, which is consistent with general findings regarding the performances of QPscGW for normal sp semiconductors [77].

B. f-electron oxides with $4f^0$ configuration: La_2O_3 and CeO_2

We next consider f-electron oxides with an empty f shell, using CeO_2 and La_2O_3 as the representatives. We first use CeO_2 to check the effects of including HLOs on the main electronic band structure features, and then compare numerically converged GW results to experiment for two f^0 compounds CeO_2 and La_2O_3.

For CeO_2, the main quantities of interest are the band gap between the valence band with dominant O-2p characters and the unoccupied 4f states, denoted as $E_{\rm g}^{\rm (p-f)}$, the band gap between the O-2p VB and unoccupied Ce-5d states, denoted as $E_{\rm g}^{\rm (p-d)}$, and the GW correction to the VBM ($\Delta\mathcal{E}_{\rm VBM}$). Figure 2 shows the evolution of the values of $E_{\rm g}^{\rm (p-f)}$, $E_{\rm g}^{\rm (p-d)}$, and $\Delta\mathcal{E}_{\rm VBM}$ as a function of $n_{\rm LO}$ and $l_{\rm max}^{\rm (LO)}$. When using the default $l_{\rm max}^{\rm (LO)}$, both $E_{\rm g}^{\rm (p-f)}$ and $E_{\rm g}^{\rm (p-d)}$ increase significantly when $n_{\rm LO}$ increases from 0 to 1, but become nearly constant as $n_{\rm LO}$ further increases, and their finally converged values are about 0.2 and 0.4 eV larger than those obtained with $n_{\rm LO} = 0$, respectively, which is a relatively milder effect compared to that observed in systems like ZnO [26]. More significant effects are observed when increasing $l_{\rm max}^{\rm (LO)}$: while $E_{\rm g}^{\rm (p-d)}$ increases moderately by about 0.3 eV, the value of $E_{\rm g}^{\rm (p-f)}$ decreases significantly by as much as 0.9 eV when $l_{\rm max}^{\rm (LO)}$ increases from $l_{\rm max}^{\rm (v)}$ to $l_{\rm max}^{\rm (v)} + 5$. Obviously including HLOs to higher angular momentum channels can significantly push unoccupied 4f states towards lower energy.

Figure 3 shows the density of states of CeO_2 and La_2O_3 from GW_0@PBE+U using the the default LAPW and LAPW+HLOs, respectively, compared to experiment. The most pronounced feature of these plots is that inclusion of HLOs shifts the position of unoccupied 4f states

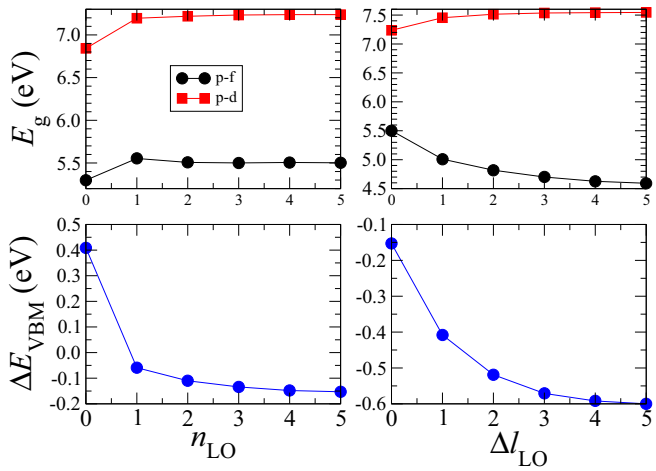

FIG. 2. Convergence of the G_0W_0@PBE band gap (E_g, upper panels), including both ($E_g^{(p-f)}$) and $E_g^{(p-d)}$, and the quasiparticle correction to VBM ($\Delta\mathcal{E}_{VBM}$, lower panels) of CeO_2 (using $N_k = 2\times2\times2$) as a function of n_{LO} [left panels, with $l_{max}^{(LO)} = l_{max}^{(LO)}(def)$] and Δl_{LO} in $l_{max}^{(LO)} = l_{max}^{(v)} + \Delta l_{LO}$ (right panels, with $n_{LO} = 5$), respectively.

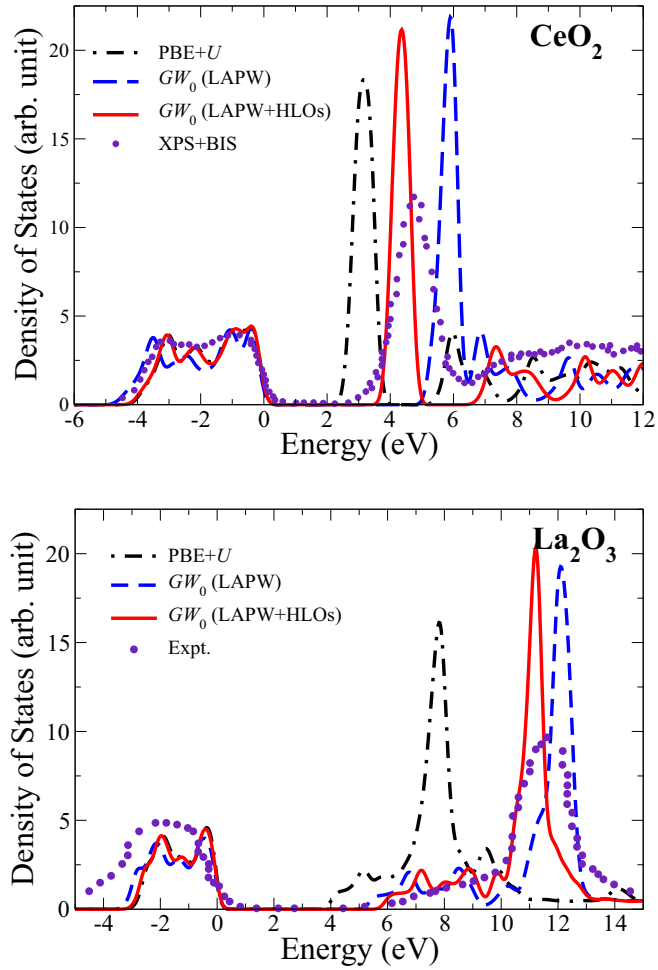

FIG. 3. Density of states of CeO_2 (upper panel) and La_2O_3 (lower panel) from GW_0@PBE+U using the the default LAPW ($n_{LO} = 0$) and LAPW+HLOs ($n_{LO} = 5$ and $l_{max}^{(LO)} = l_{max}^{(v)} + 4$), respectively, compared to experiment. The experimental spectral data measured from the x-ray photoelectron spectroscopy (XPS) and bremmsstrahlung isochromat spectroscopy (BIS) for CeO_2 and La_2O_3 are taken from Refs. [85,86], respectively.

towards lower energy, as we have discussed above. Comparing theory to experiment, we can see that for CeO_2, GW_0@PBE+U with the default LAPW basis overestimates the energy of unoccupied $4f$ states (f^{unocc}) significantly. The resultant band gap of 5.2 eV, as shown in Table II, is therefore also significantly overestimated compared to experimental values. After considering HLOs, f^{unocc} states are significantly shifted towards lower energy by about 2 eV, and the predicted f^{unocc} peak position agrees well with experiment.

Similar features can also be observed in La_2O_3, in which f^{unocc} states fall energetically above the conduction band minimum and the fundamental band gap is formed between O-$2p$ dominant valence band and the La-$5d$ dominant conduction band. The consideration of HLOs increases the GW_0 (G_0W_0) band gap by about 0.6 (0.5) eV, and shifts the position of f^{unocc} states towards lower energy by about 1 eV, which is less dramatic than that in CeO_2, probably due to the more delocalized nature of f^{unocc} states in La_2O_3. With the LAPW+HLOs basis, both G_0W_0 and GW_0 band gaps fall in the range of experimental values.

Overall we can see that the inclusion of HLOs improve the agreement between GW prediction and experiment both in terms of the band gap and the position of f^{unocc} states for f oxides with an empty f shell.

C. f^n systems: Ce_2O_3 and UO_2

We further consider f-electron oxides with partially occupied f shell, Ce_2O_3 and UO_2. In Ce_2O_3, the minimal band gap is formed between the occupied $4f^1$ states and the unoccupied Ce-$5d$ states. In our previous study [35] we found that when comparing the G_0W_0@LDA+U results to the experimental photoemission spectral data, the energy splitting between the occupied $4f^1$ states and the O-$2p$ valence bands are significantly overestimated. In other words, the GW approach tends to underestimate the binding energy of highly localized $4f$ states, which has been also observed in other f-electron systems such as UO_2, PuO_2, and Pu_2O3 in our calculations. As shown in Fig. 4, when using $l_{max}^{(LO)} = l_{max}^{(LO)}(def)$, increasing n_{LO} from 0 to 5 only moderately increases the minimal f-d gap by about 0.2 eV, and $\Delta\mathcal{E}_{VBM}$ is reduced by about 0.5 eV. It is noteworthy that $\Delta\mathcal{E}_{VBM}$ remains to be positive even with $n_{LO} = 5$, indicating that the GW correction pushes the VBM towards higher energy rather than lower energy, which is opposite to the general trend typically observed in sp insulating systems [24,26]. In addition, the splitting between $4f^1$ and the O-$2p$ VB, denoted as Δ_{p-f}, which is characterized by the energy of the upper edge of the O-$2p$ VB with respect to the energy of the highest occupied $4f$ state, is also slightly increased. When keeping $n_{LO} = 5$ and adding HLOs to higher angular momentum channels by increasing Δl_{LO} from 0 to 5, all those three quantities have been dramatically modified: the f-d gap increases by almost 1.3 eV, and $\Delta\mathcal{E}_{VBM}$ decreases by 1.3 eV and becomes negative. From the fact that the magnitude of the change in E_g and $\Delta\mathcal{E}_{VBM}$ is essentially the same, one can see that the opening of the gap is mainly due to the shift

TABLE II. Band gaps of f-electron oxides from PBE+U, G_0W_0@PBE+U, and GW_0@PBE+U at different levels of numerical accuracy compared to experiment. The columns with LAPW are the results obtained from using the default LAPW basis ($n_{\rm LO}=0$), and those with LAPW+HLOs are the results obtained with $n_{\rm LO}=5$ and $l_{\rm max}^{\rm (LO)}=l_{\rm max}^{\rm (v)}+4$ for La_2O_3 and CeO_2, $n_{\rm LO}=7$ and $l_{\rm max}^{\rm (LO)}=l_{\rm max}^{\rm (v)}+5$ for Ce_2O_3, and $n_{\rm LO}=4$ and $l_{\rm max}^{\rm (LO)}=l_{\rm max}^{\rm (v)}+4$ for UO_2, respectively. The values of U and J are obtained from constrained DFT calculations.

			G_0W_0		GW_0		
System	U,J	PBE+U	LAPW	LAPW+HLOs	LAPW	LAPW+HLOs	Expt.
La_2O_3	6.1, 0.7	3.92	4.91	5.41	5.18	5.80	5.55,[a] 5.3,[b] 5.5–5.9[c]
CeO_2	6.1, 0.7	2.63	4.35	3.62	5.23	3.88	3.3,[d] 3.78[e]
Ce_2O_3	6.1, 0.7	2.21	1.78	3.35	1.43	3.57	2.4[a]
UO_2	4.1, 0.0	2.15	2.28	2.73	2.29	2.87	2.1,[f] 2.7,[g] 2.5[h]

[a]Reference [78].
[b]Reference [79].
[c]Reference [80].
[d]Reference [81].
[e]Reference [82].
[f]Reference [53].
[g]Reference [83].
[h]Reference [84].

of the $4f^1$ states towards lower energy. The latter is also the main cause for the shrinkage of the splitting between the occupied $4f^1$ states and O-$2p$ VB states by nearly 1 eV, as indicated by the decreasing value of $\Delta_{\rm p-f}$ with increasing $\Delta l_{\rm LO}$. Overall one can see that adding HLOs of large angular quantum numbers can dramatically push occupied $4f$ states towards lower energy.

Using numerically converged parameters we performed G_0W_0 and GW_0@PBE+U calculations for Ce_2O_3 and UO_2. In Fig. 5 we compare density of states from PBE+U and GW_0@PBE+U using the the default LAPW and

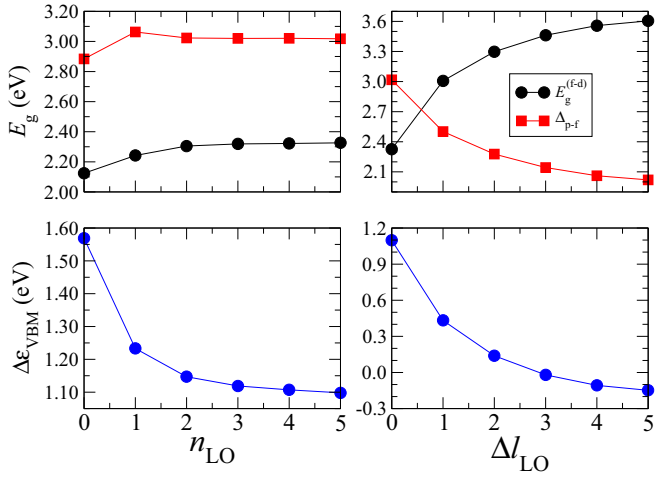

FIG. 4. Convergence of the G_0W_0@PBE+U band gap (E_g, upper panels), and the quasiparticle correction to VBM ($\Delta\mathcal{E}_{\rm VBM}$, lower panels) of Ce_2O_3 as a function of $n_{\rm LO}$ [left panels, with $l_{\rm max}^{\rm (LO)}=l_{\rm max}^{\rm (LO)}$(def)] and $\Delta l_{\rm LO}$ in $l_{\rm max}^{\rm (LO)}=l_{\rm max}^{\rm (v)}+\Delta l_{\rm LO}$ (right panels, with $n_{\rm LO}=5$), respectively, calculated by using $N_k=2\times2\times1$ and PBE+U with $U=6.8$ eV and $J=0.0$ eV as the starting point. In the upper panels, the splitting between the O-$2p$ valence band upper edge and the highest occupied $4f$ state energy ($\Delta_{\rm p-f}$) is also shown.

LAPW+HLOs, respectively, to experimental photoemission spectral data.

For Ce_2O_3, apparently PBE+U gives a rather good description of some features of electronic band structure, including a fundamental band gap of 2.21 eV that is very close to the experimental value of 2.4 eV (see the data in Table II), and the splitting between O-$2p$ and $f^{\rm occ}$ is only slightly underestimated. But the position of $f^{\rm unocc}$ states is dramatically underestimated by about 4 eV, which indicates that PBE+U by itself is not adequate to give an accurate description of electronic band structure of strongly correlated systems [36]. When using the standard LAPW basis, GW_0 significantly overestimates the splitting between O-$2p$ and Ce-4 $f^{\rm occ}$ states ($\Delta_{\rm p-f}$), and significantly underestimates the fundamental band gap, by about 1 eV compared to the experimental value. When using the LAPW+HLOs basis, the GW_0 description of $\Delta_{\rm p-f}$ is significantly improved and now both the positions of occupied and unoccupied $4f$ states agree well with those indicated in the experimental spectral data. In the meanwhile, the fundamental band gap increases by more than 2 eV as a result of including HLOs.

Compared to the experimental value of 2.4 eV, the GW_0 band gap with the LAPW+HLOs basis is overestimated by about 1.2 eV. It is worthwhile to have a closer look at the reliability of the experimental band gap of Ce_2O_3. Compared to other lanthanide sesquioxides, the band gap of Ce_2O_3 has been scarcely measured and reported, due to the difficulty to grow stoichiometric single crystals [78]. The widely cited value of 2.4 eV was obtained from optical absorption measurement [78], and the possible role played by excitonic effects has never been addressed, as far as we know. In principle, direct and inverse photoemission spectroscopy is the more straightforward way to obtain the fundamental band gap. In Fig. 5 two sets of experimental data for Ce_2O_3 are collected, one from the XPS-BIS measurement [76], and the other one from XPS plus x-ray absorption spectroscopy (XAS) [88]. Considering that the energy zero is defined differently in experimental spectral data and theoretical DOS, we align the experimental

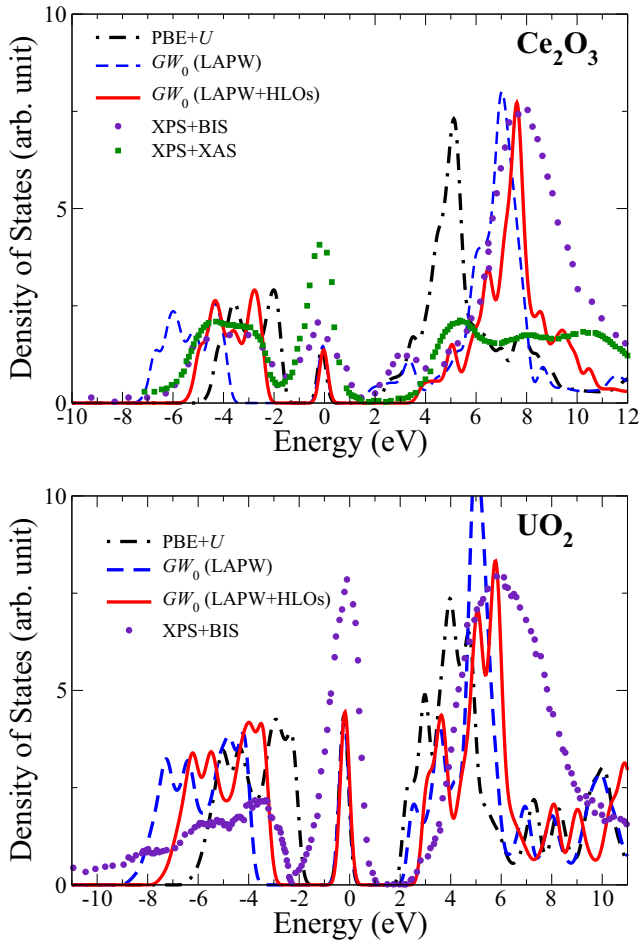

FIG. 5. Density of states of Ce_2O_3 (upper panel) and UO_2 (lower panel) from PBE+U and GW_0@PBE+U using the the default LAPW and LAPW+HLOs, respectively, compared to experiment. The experimental spectral data measured from the x-ray photoelectron spectroscopy (XPS) and bremmsstrahlung isochromat spectroscopy (BIS) for Ce_2O_3 and UO_2 are taken from Refs. [76,87], respectively. We also show for Ce_2O_3 the experimental spectral data measured by combining XPS with x-ray absorption spectroscopy (XPS+XAS) taken from [88].

data with theoretical ones in the terms of the peak position of the occupied f states. We note that a different treatment was used in Ref. [35], in which the alignment was done in terms of the upper edge of O-2p valence band. Obviously using different alignment convention should have no influences on physical implications of such comparison. Since our new GW calculations with LAPW+HLOs predict the splitting between O-2p and $f^{\rm occ}$ in good agreement with experiment, two alignment schemes lead to essentially the same result. It is also important to note that the shoulder peak at about 3 eV in the XPS+BIS spectral data can be attributed to the residual CeO_2 in the Ce_2O_3 sample, which can be clearly seen from the evolution of the spectral data as the measured sample is gradually reduced from CeO_2 to Ce_2O_3 shown in Fig. 3 of Ref. [76]. That feature overlaps with the lower edge of the Ce-5d dominant conduction band, such that it is difficult to extract the fundamental gap of Ce_2O_3 from the XPS+BIS data. This interpretation of the XPS+BIS result is supported by the XPS+XAS spectral data in which no peak around the conduction band bottom is present. Combining the XPS+BIS and XPS+XAS data, we can clearly see that the true fundamental gap of Ce_2O_3 should be significantly larger than 2.4 eV. The fact that the GW_0 DOS agrees very well with the XPS+XAS data in the region around the CB bottom indicates that the GW_0 band gap (3.6 eV) obtained with LAPW+HLOs basis should be very close to the exact one.

We next consider the actinide oxide UO_2 with the partially occupied 5f shell, which exhibits similar features as Ce_2O_3. GW_0 with the standard LAPW basis again overestimates the splitting between O-2p and U-5f states, and considering HLOs reduces the splitting by about 1 eV. With LAPW+HLOs basis, GW_0 can well reproduce all main features of the experimental spectral data, including, in particular, the positions of occupied and unoccupied 5f states. For the band gap, including HLOs increases the GW_0 band gap by about 0.6 eV, and a slightly smaller change occurs for the G_0W_0 band gap. Comparing the results for Ce_2O_3 and UO_2, we can see that the overall effect of HLOs is significant weaker for 5f states than for 4f states. The experimental band gap of UO_2 is likely to be impaired by similar uncertainty as Ce_2O_3 and scatters in the range of 2.1–2.7 eV. The GW_0 band gap with LAPW+HLOs is about 2.9 eV, which is reasonably close to the experimental values.

IV. CONCLUDING REMARKS

In this work we have revisited the topic of the GW approach to d- and f-electron oxides [35,36] based on a numerically accurate implementation of the all-electron GW method with the high-energy local-orbitals enhanced LAPW (LAPW+HLOs) basis [26]. We have found that the inclusion of HLOs has significantly stronger effects on GW quasiparticle electronic band structure of d- and f-electron oxides than it does of typical normal sp insulating systems [26]. In particular, the features related to localized d or f states in the electronic band structure of these compounds are more strongly affected than those related to itinerant states, and are significantly improved when comparing with experimental results. Based on numerically accurate calculations, we have demonstrated that using the DFT+U as the starting point, GW_0 can well describe electronic band structure of d- and f-electron oxides. Based on a careful comparison between GW_0 density of states with experimental spectral data, we think that the widely cited experimental band gap of Ce_2O_3 (2.4 eV) may well have significant errors, and our predicted result (3.6 eV) from numerically converged GW_0@PBE+U should be close to the correct value.

The findings presented in this work from numerically accurate GW calculations have clearly indicated that with a qualitatively correct description of d- or f-electron systems by the Hubbard U corrected local or semilocal density approximations as the starting point, the GW approach in the G_0W_0 or GW_0 scheme can describe the electronic band structure of strongly correlated systems with a much better accuracy than previously reported or expected. Since our study focuses on quasiparticle electronic band structure, its treatment of strong correlation is still limited to some extent. For one thing, other strong correlation features such as satellite structures in PES

[71], dynamical fluctuation of magnetic moment, to name a few only, are still out of reach, and requires extending to a more general theoretical framework such as the combination of GW with dynamical mean field theory (GW+DMFT) [89–91]. One of the key messages of this work is the importance of numerical accuracy in GW-like calculations, and we believe that any further physical consideration beyond GW should be based on numerically accurate treatment at the GW level. Although the computational cost increases as a result of including HLOs, the outcome provides a more consistent picture regarding the accuracy of the GW approach in general for both simple sp insulators and strongly correlated d- or f-electron systems, which provide a more solid base for further development of first-principles approaches to strongly correlated systems [90,92–94].

ACKNOWLEDGMENT

This work is partly supported by the National Natural Science Foundation of China (21673005, 21621061).

[1] G. Onida, L. Reining, and A. Rubio, Rev. Mod. Phys. **74**, 601 (2002).
[2] P. Liao and E. A. Carter, Chem. Soc. Rev. **42**, 2401 (2013).
[3] Y. Ping, D. Rocca, and G. Galli, Chem. Soc. Rev. **42**, 2437 (2013).
[4] C. Di Valentin, S. Botti, and M. Cococcioni, Eds., *First Principles Approaches to Spectroscopic Properties of Complex Materials*, Vol. 347 of Topics in Current Chemistry (Springer, Heidelberg, 2014).
[5] L. Hedin, Phys. Rev. **139**, A796 (1965).
[6] M. S. Hybertsen and S. G. Louie, Phys. Rev. B **34**, 5390 (1986).
[7] R. W. Godby, M. Schlüter, and L. J. Sham, Phys. Rev. B **37**, 10159 (1988).
[8] F. Aryasetiawan and O. Gunnarsson, Rep. Prog. Phys. **61**, 237 (1998).
[9] W. G. Aulbur, L. Jönsson, and J. W. Wilkins, Solid State Phys. **54**, 1 (2000).
[10] H. N. Rojas, R. W. Godby, and R. J. Needs, Phys. Rev. Lett. **74**, 1827 (1995).
[11] M. Rohlfing, P. Krüger, and J. Pollmann, Phys. Rev. B **48**, 17791 (1993).
[12] X. Blase, C. Attaccalite, and V. Olevano, Phys. Rev. B **83**, 115103 (2011).
[13] S. Lebègue, B. Arnaud, M. Alouani, and P. E. Bloechl, Phys. Rev. B **67**, 155208 (2003).
[14] M. Shishkin and G. Kresse, Phys. Rev. B **74**, 035101 (2006).
[15] F. Hüser, T. Olsen, and K. S. Thygesen, Phys. Rev. B **87**, 235132 (2013).
[16] F. Aryasetiawan, Phys. Rev. B **46**, 13051 (1992).
[17] W. Ku and A. G. Eguiluz, Phys. Rev. Lett. **89**, 126401 (2002).
[18] T. Kotani and M. van Schilfgaarde, Solid State Commun. **121**, 461 (2002).
[19] M. Usuda, N. Hamada, T. Kotani, and M. van Schilfgaarde, Phys. Rev. B **66**, 125101 (2002).
[20] C. Friedrich, A. Schindlmayr, S. Blügel, and T. Kotani, Phys. Rev. B **74**, 045104 (2006).
[21] M. van Schilfgaarde, T. Kotani, and S. V. Faleev, Phys. Rev. B **74**, 245125 (2006).
[22] R. Gomez-Abal, X. Li, M. Scheffler, and C. Ambrosch-Draxl, Phys. Rev. Lett. **101**, 106404 (2008).
[23] C. Friedrich, S. Blügel, and A. Schindlmayr, Phys. Rev. B **81**, 125102 (2010).
[24] H. Jiang, R. I. Gomez-Abal, X. Li, C. Meisenbichler, C. Ambrosch-Draxl, and M. Scheffler, Comput. Phys. Commun. **184**, 348 (2013).
[25] I.-H. Chu, A. Kozhevnikov, T. C. Schulthess, and H.-P. Cheng, J. Chem. Phys. **141**, 044709 (2014).
[26] H. Jiang and P. Blaha, Phys. Rev. B **93**, 115203 (2016).
[27] D. Nabok, A. Gulans, and C. Draxl, Phys. Rev. B **94**, 035118 (2016).
[28] X. Ren, P. Rinke, V. Blum, J. Wieferink, A. Tkatchenko, A. Sanfilippo, K. Reuter, and M. Scheffler, New J. Phys. **14**, 053020 (2012).
[29] B.-C. Shih, Y. Xue, P. Zhang, M. L. Cohen, and S. G. Louie, Phys. Rev. Lett. **105**, 146401 (2010).
[30] M. Stankovski, G. Antonius, D. Waroquiers, A. Miglio, H. Dixit, K. Sankaran, M. Giantomassi, X. Gonze, M. Côté, and G.-M. Rignanese, Phys. Rev. B **84**, 241201(R) (2011).
[31] C. Friedrich, M. C. Müller, and S. Blügel, Phys. Rev. B **83**, 081101(R) (2011).
[32] A. Grüneis, G. Kresse, Y. Hinuma, and F. Oba, Phys. Rev. Lett. **112**, 096401 (2014).
[33] R. Laskowski and P. Blaha, Phys. Rev. B **85**, 035132 (2012).
[34] Y. Hinuma, A. Grüneis, G. Kresse, and F. Oba, Phys. Rev. B **90**, 155405 (2014).
[35] H. Jiang, R. I. Gomez-Abal, P. Rinke, and M. Scheffler, Phys. Rev. Lett. **102**, 126403 (2009).
[36] H. Jiang, R. I. Gomez-Abal, P. Rinke, and M. Scheffler, Phys. Rev. B **82**, 045108 (2010).
[37] H. Jiang, P. Rinke, and M. Scheffler, Phys. Rev. B **86**, 125115 (2012).
[38] S. Lany, Phys. Rev. B **87**, 085112 (2013).
[39] P. Liao and E. A. Carter, Phys. Chem. Chem. Phys. **13**, 15189 (2011).
[40] M. C. Toroker, D. K. Kanan, N. Alidoust, L. Y. Isseroff, P. Liao, and E. A. Carter, Phys. Chem. Chem. Phys. **13**, 16644 (2011).
[41] C. E. Patrick and F. Giustino, J. Phys.: Condens. Matter **24**, 202201 (2012).
[42] Z. Ergönenc, B. Kim, P. Liu, G. Kresse, and C. Franchini, Phys. Rev. Mater. **2**, 024601 (2018).
[43] R. Laskowski and P. Blaha, Phys. Rev. B **89**, 014402 (2014).
[44] Z.-H. Cui and H. Jiang, Phys. Chem. Chem. Phys. **18**, 29914 (2016).
[45] J. Klimes, M. Kaltak, and G. Kresse, Phys. Rev. B **90**, 075125 (2014).
[46] K. Terakura, T. Oguchi, A. R. Williams, and J. Kübler, Phys. Rev. B **30**, 4734 (1984).
[47] K. N. Kudin, G. E. Scuseria, and R. L. Martin, Phys. Rev. Lett. **89**, 266402 (2002).
[48] I. D. Prodan, G. E. Scuseria, and R. L. Martin, Phys. Rev. B **73**, 045104 (2006).

[49] L. E. Roy, T. Durakiewicz, R. L. Martin, J. E. Peralta, G. E. Scuseria, C. G. Olson, J. J. Joyce, and E. Guziewicz, J. Comput. Chem. **29**, 2288 (2008).

[50] H. He, D. A. Andersson, D. D. Allred, and K. K. Rector, J. Phys. Chem. C **117**, 16540 (2013).

[51] F. Tran, P. Blaha, K. Schwarz, and P. Novak, Phys. Rev. B **74**, 155108 (2006).

[52] L. Eyring, *The Binary Rare Earth Oxides*, Handbook on the Physics and Chemistry of Rare Earths (North-Holland, Amsterdam, 1979), Chap. 27, Vol. 3, p. 337.

[53] J. Schoenes, J. Appl. Phys. **49**, 1463 (1978).

[54] P. Blaha, K. Schwarz, G. K. H. Madsen, D. Kvasnicka, and J. Luitz, *WIEN2k, An Augmented Plane Wave + Local Orbitals Program for Calculating Crystal Properties* (Karlheinz Schwarz, Techn. Universität Wien, Austria, 2001).

[55] G. K. H. Madsen, P. Blaha, K. Schwarz, E. Sjöstedt, and L. Nordström, Phys. Rev. B **64**, 195134 (2001).

[56] See Supplemental Material at http://link.aps.org/supplemental/10.1103/PhysRevB.97.245132 for additional computational details and data.

[57] J. P. Perdew, K. Burke, and M. Ernzerhof, Phys. Rev. Lett. **77**, 3865 (1996).

[58] V. I. Anisimov and O. Gunnarsson, Phys. Rev. B **43**, 7570 (1991).

[59] G. K. H. Madsen and P. Novak, Europhys. Lett. **69**, 777 (2005).

[60] D. J. Singh and L. Nordström, *Planewaves, Pseudopotentials and the LAPW Method*, 2nd ed. (Springer, New York, 2006).

[61] J. van Elp, R. H. Potze, H. Eskes, R. Berger, and G. A. Sawatzky, Phys. Rev. B **44**, 1530 (1991).

[62] E. Z. Kurmaev, R. G. Wilks, A. Moewes, L. D. Finkelstein, S. N. Shamin, and J. Kunes, Phys. Rev. B **77**, 165127 (2008).

[63] H. K. Bowen, D. Adler, and B. H. Auker, J. Solid State Chem. **12**, 355 (1975).

[64] J. van Elp, J. L. Wieland, H. Eskes, P. Kuiper, G. A. Sawatzky, F. M. F. de Groot, and T. S. Turner, Phys. Rev. B **44**, 6090 (1991).

[65] M. Gvishi and D. S. Tannhauser, J. Phys. Chem. Solids **33**, 893 (1972).

[66] G. A. Sawatzky and J. W. Allen, Phys. Rev. Lett. **53**, 2339 (1984).

[67] C. Rödl, F. Fuchs, J. Furthmüller, and F. Bechstedt, Phys. Rev. B **79**, 235114 (2009).

[68] S. V. Faleev, M. van Schilfgaarde, and T. Kotani, Phys. Rev. Lett. **93**, 126406 (2004).

[69] S. Das, J. E. Coulter, and E. Manousakis, Phys. Rev. B **91**, 115105 (2015).

[70] L.-H. Ye, R. Asahi, L.-M. Peng, and A. J. Freeman, J. Chem. Phys. **137**, 154110 (2012).

[71] F. Aryasetiawan and O. Gunnarsson, Phys. Rev. Lett. **74**, 3221 (1995).

[72] S. Massidda, A. Continenza, M. Posternak, and A. Baldereschi, Phys. Rev. Lett. **74**, 2323 (1995).

[73] C. H. Patterson, Int. J. Quantum Chem. **106**, 3383 (2006).

[74] C. Rödl, F. Fuchs, J. Furthmüller, and F. Bechstedt, Phys. Rev. B **77**, 184408 (2008).

[75] M.-Y. Zhang and H. Jiang (unpublished).

[76] J. W. Allen, J. Magn. Magn. Mater. **47–48**, 168 (1985).

[77] M. Shishkin, M. Marsman, and G. Kresse, Phys. Rev. Lett. **99**, 246403 (2007).

[78] A. V. Prokofiev, A. I. Shelykh, and B. T. Melekh, J. Alloys. Compounds **242**, 41 (1996).

[79] Y. Zhao, K. Kita, K. Kyuno, and A. Toriumi, Appl. Phys. Lett. **94**, 042901 (2009).

[80] T. Das, C. Mahata, C. K. Maiti *et al.*, J. Electrochem. Soc. **159**, G15 (2012).

[81] V. V. Afanas'ev, S. Shamuilia, A. Stesmans, A. Dimoulas, Y. Panayiotatos, A. Sotiropoulos, M. Houssa, and D. P. Brunco, Appl. Phys. Lett. **88**, 132111 (2006).

[82] T. R. Griffiths, M. J. Davies, and H. V. S. A. Hubbard, J. Chem. Soc. Faraday Trans. II **72**, 765 (1976).

[83] B. W. Veal and D. J. Lam, Phys. Rev. B **10**, 4902 (1974).

[84] S. M. Gilbertson, T. Durakiewicz, G. L. Dakovski, Y. Li, J.-X. Zhu, S. D. Conradson, S. A. Trugman, and G. Rodriguez, Phys. Rev. Lett. **112**, 087402 (2014).

[85] E. Wuilloud, B. Delley, W.-D. Schneider, and Y. Baer, Phys. Rev. Lett. **53**, 202 (1984).

[86] W.-D. Schneider, B. Delley, E. Wuilloud, J.-M. Imer, and Y. Baer, Phys. Rev. B **32**, 6819 (1985).

[87] Y. Baer and J. Schoenes, Solid State Commun. **33**, 885 (1980).

[88] D. R. Mullins, S. H. Overbury, and D. R. Huntley, Surf. Sci. **409**, 307 (1998).

[89] S. Biermann, F. Aryasetiawan, and A. Georges, Phys. Rev. Lett. **90**, 086402 (2003).

[90] S. Biermann, J. Phys.: Condens. Matter **26**, 173202 (2014).

[91] F. Nilsson, L. Boehnke, P. Werner, and F. Aryasetiawan, Phys. Rev. Mater. **1**, 043803 (2017).

[92] H. Jiang, Int. J. Quantum Chem. **115**, 722 (2015).

[93] F. Lechermann, A. I. Lichtenstein, and M. Potthoff, Eur. Phys. J. Special Topics **226**, 2591 (2017).

[94] M. Imada and T. Miyake, J. Phys. Soc. Jpn. **79**, 112001 (2010).